Spectral and spatial contributions to white light generation from InGaN/GaN dot-in-a-wire nanostructures

Yousef Kamali, Brenna R. Walsh, Jonathan Mooney, Hieu Nguyen, Colin Brosseau, Richard Leonelli, Zetian Mi, and Patanjali Kambhampati

Citation: Journal of Applied Physics **114**, 164305 (2013); doi: 10.1063/1.4826618
View online: http://dx.doi.org/10.1063/1.4826618
View Table of Contents: http://scitation.aip.org/content/aip/journal/jap/114/16?ver=pdfcov
Published by the AIP Publishing

Spectral and spatial contributions to white light generation from InGaN/GaN dot-in-a-wire nanostructures

Yousef Kamali,[1,2] Brenna R. Walsh,[1] Jonathan Mooney,[1] Hieu Nguyen,[3] Colin Brosseau,[4] Richard Leonelli,[4] Zetian Mi,[3] and Patanjali Kambhampati[1,a)]
[1]*Department of Chemistry, McGill University, Montreal H3A 2K6, Canada*
[2]*Department of Physics, Faculty of Science, University of Mohaghegh Ardabili, P.O. Box 179 Ardabil, Iran*
[3]*Department of Electrical and Computer Engineering, McGill University, Montreal H3A 0E9, Canada*
[4]*Department of Physics, Université de Montreal, Montreal H3C 3J7, Canada*

(Received 18 July 2013; accepted 7 October 2013; published online 23 October 2013)

We analyze epitaxially grown InGaN/GaN dot-in-a-wire heterostructures to relate growth and design properties to trends seen in photoluminescence (PL) and resonance Raman spectra. Temperature-dependent PL measurement of these dot-in-a-wire heterostructures illustrate an expected decrease in integrated PL emission and an unusual narrowing of peak width with increasing temperature. Information extracted from Resonance Raman spectra was utilized in a time-dependent model to analyze and to simulate PL spectra. These spectra were found to be in good agreement with the experimental PL data and provided insight into the broadening mechanisms affecting the samples. PL measurements were taken as a function of position on the sample and radial variation of peak energies was observed. This variation was attributed to the radial temperature gradient present during nanowire growth. These additional characteristics of the nanowire heterostructures will allow for increased understanding of these systems potentials for applications in white light emitting diodes. © *2013 AIP Publishing LLC*. [http://dx.doi.org/10.1063/1.4826618]

I. INTRODUCTION

In recent years, the potential applications for nanowire heterostructures in optoelectronic devices,[1,2] such as solar cells,[3,4] light emitting diodes (LEDs),[5–7] lasers,[8,9] sensors,[10,11] and photodetectors,[2,12] have been widely investigated. In particular, there has been a growing demand for low-cost, high-efficiency, phosphor-free white light LEDs that can be made on a single chip.[13] Epitaxially grown GaN nanowire heterostructures offer reduced defect densities and strain distribution, due to the effective lateral stress relaxation.[14] In addition, the nanowire structures can improve light extraction efficiency due to the large surface-to-volume ratios.[15,16]

Recently, InGaN/GaN dot-in-a-wire heterostructures grown by radio frequency plasma-assisted molecular beam epitaxy (MBE) have shown high light extraction efficiency for white light emission.[17] Quantum dots (QDs) embedded in the GaN nanowire matrix have three dimensional carrier confinement. This growth method allows for a high degree of emission wavelength tunability by varying Indium composition ($In_{1-x}Ga_x$) and quantum dot size.

To fully exploit potential applications in optoelectronic devices, further study on the spectral properties of these dot-in-a-wire heterostructures is needed. The photoluminescence (PL) and electroluminescence (EL) of InGaN/GaN dot-in-a-wire nanostructures were recently investigated at room temperature.[18,19] We expand on these initial works by examining temperature dependence of the PL spectra, variation in spectral properties as a function of wafer position, and resonance Raman intensity analysis.

Raman spectroscopy plays an important role in optical characterization of semiconductors.[20] Parameters such as band frequencies and intensities, line shape, and linewidth can be extracted from Raman spectra. We present room temperature resonance Raman spectra of InGaN/GaN dot-in-a-wire heterostructures and employ information obtained from them to model the corresponding PL spectrum. These experiments reveal two contributions to the origin of the spectral width: homogenous broadening via phonon coupling, and inhomogeneous broadening due to growth conditions.

II. EXPERIMENT

InGaN/GaN dot-in-a-wire heterostructures were epitaxially grown on Si(111) substrates. The details of the growth procedure can be found elsewhere.[19,21] Here, we present two heterostructures with different quantum dot environments. Both systems consist of GaN nanowires grown perpendicular to the Si surface; one system has one InGaN quantum dot per nanowire, while in the other there are ten InGaN quantum dots vertically stacked in each GaN nanowire (Fig. 1). For the remainder of the paper, we will refer to these two systems as the one dot and ten dot samples. Each dot has a height of ~3 nm and in the ten dot sample have a GaN barrier layer between dots. Quantum dots are completely confined within the GaN nanowires.

The temperature dependent PL spectra were collected with a FluoroMax-2 spectrometer. The excitation wavelength was 405 nm (photon energy of 3.06 eV), and the emission wavelength was scanned from 415 to 800 nm. A Janis (STVP-100) flow cryostat was used to cool the wafer between 300 and 80 K.

a)Author to whom correspondence should be addressed. Electronic mail: pat.kambhampati@mcgill.ca.

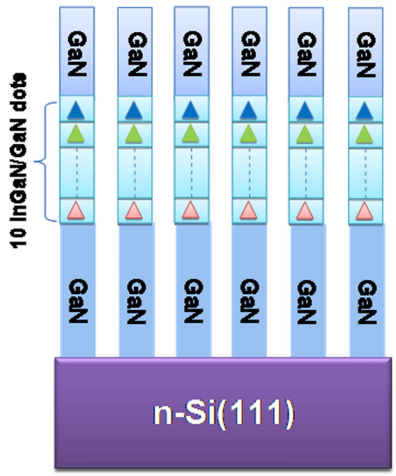

FIG. 1. Schematic diagram of 10 InGaN/GaN dots. GaN nanowires are grown on the (111) surface of Si wafers. InGaN QDs are represented by triangles in the center of the nanowires. The above figure represents a 10 InGaN QD system, but variability in quantum dot number per nanowire in different samples is represented by dashed lines in QD region.

Photoluminescence spectra were also measured across the surface of the sample. A 445 nm diode laser was used to take PL measurements every 2 mm in a grid pattern both vertically and horizontally, allowing us to create a PL "map" of the sample. The Jacobian transform was used to convert all absorption and PL measurements from wavelength to energy units (eV).

Resonance Raman spectra were collected at room temperature (292 K) using a frequency doubled CW Ti:sapphire laser system with excitation wavelength of 362.3 nm (photon energy of 3.42 eV) and power of 80–90 mW. The beam was focused on the sample resulting in an intensity of about 5×10^3 W/cm^2. The Raman signal was detected with a cooled Princeton Instruments CCD (ST133 Controller) connected to a 0.5 m Jobin Yvon Double Raman (U1000) spectrometer.

III. RESULTS AND DISCUSSION

Photoluminescence spectra at room temperature for both one and ten dot samples are shown in Fig. 2. Their peak emission energies are 2.167 and 2.198 eV and their full width at half maximum (FWHM) values are 282 and 413 meV, respectively. The FWHM values include contributions from both homogeneous and inhomogeneous broadenings. The homogeneous linewidths are expected to be same for both samples as they are intrinsic to the system; however, the ten dot sample should have a larger inhomogeneous linewidth because it includes a distribution of quantum dot sizes.

Figures 3(a) and 3(b) show the temperature dependent PL spectra for both one and ten dot-in-a-wire samples, respectively. The integrated peak value (Fig. 3(c)) and FWHM (Fig. 3(d)) of the PL signal with temperature are also plotted, both properties decreasing with the increasing temperature. While the reduction in integrated peak area with temperature is expected,[22] the reduction of FWHM is

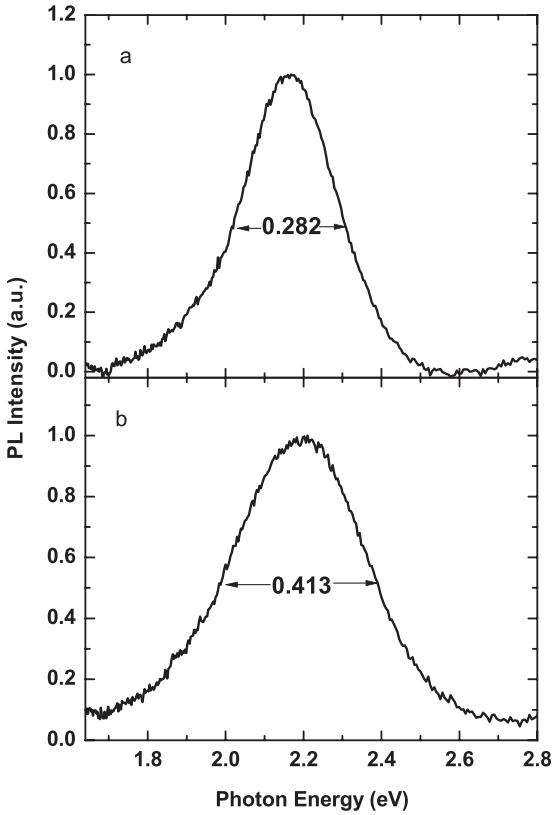

FIG. 2. Photoluminescence spectra of (a) 1 dot sample and (b) 10 dot samples, respectively. Full width half maximum values are shown.

uncommon.[23,24] The temperature dependence of PL can be qualitatively understood as arising from thermal escape of excitations from dots at higher temperatures, which inhibits radiative recombination.[23,24] A similar explanation can be invoked to explain the unusual decrease in the FWHM of the sample with increasing temperature. It has been proposed in the literature that there is a uniform energy barrier to the wetting layer, such that the activation energy required for escape will vary from dot to dot based on the size distribution.[25] Thus, as temperature increases, excitons at shallow potential minima can more easily be thermally activated, resulting in escape from these dots. The result is that as temperature increases, the contributions to higher energies in the PL spectrum are most efficiently removed, resulting in a decrease in FWHM.[25] In addition, in the case of the ten dot-in-a-wire sample, carrier hopping between dots results in a flow of carriers to dots with higher binding energies,[26] as does the greater likelihood of tunneling out of smaller dots,[27] resulting in a narrowing of the PL spectrum from the high-energy side greater than that expected for one dot-in-a-wire sample (Fig. 3).

Next, Raman spectra were obtained for both samples. After subtraction of the PL background, clear Raman peaks of fundamental, and first overtone of the longitudinal optical (LO) phonon modes are visible in the spectra of both samples at about 730 cm^{-1} and 1460 cm^{-1}. These peaks were fit to Gaussian functions. Both experimental data and fits are presented in Fig. 4(a). The single intensity of the LO phonon modes of the InGaN alloy is resonantly enhanced via the

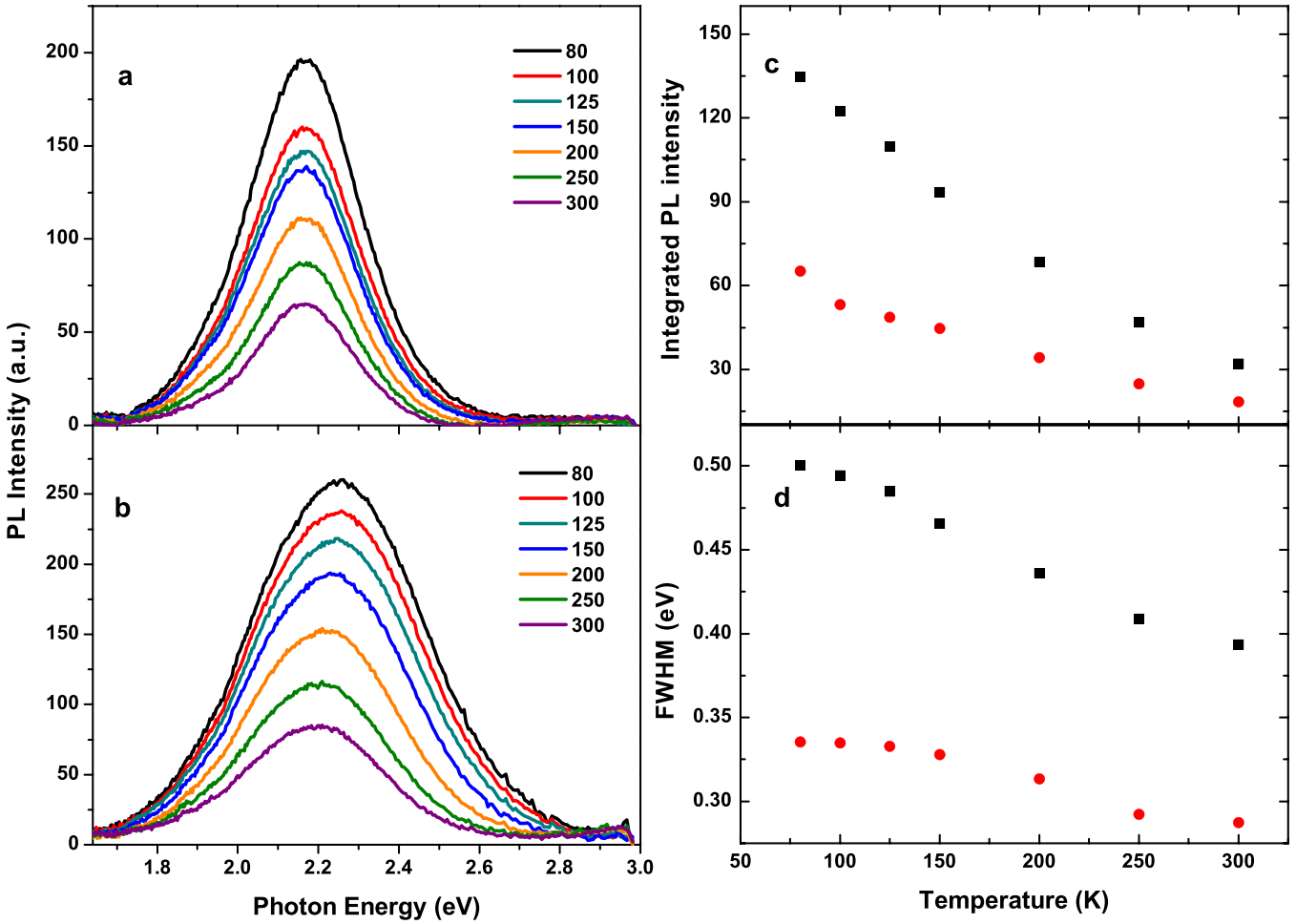

FIG. 3. Time dependent PL spectra for (a) 1 dot and (b) 10 dot-in-a-wire samples. Integrated peak area (c) and FWHM (d) of the photoluminescence with temperature, black squares 10 dot sample and red circle 1 dot sample.

Fröhlich interaction under the near resonant conditions of the experiment.[28,29] The ratios of overtone to fundamental integrated intensities were determined to be 0.439 and 0.576 for one and ten dot-in-a-wire samples, respectively.

To gain insight into the physical properties of system, time-dependent modeling of the resonance Raman intensities was accomplished by using the Raman cross section formula,[30]

$$\sigma_{0\to m}(E_l) \propto E_s^3 E_l \left| \int_0^{+\infty} e^{\frac{1}{\hbar}[i(E_l-E_0)t-\Gamma t]} S^{\frac{m}{2}} (-1)^m (m!)^{-\frac{1}{2}} \times (e^{-i\omega t}-1)^m e^{[-S(1-e^{-i\omega t})]} dt \right|^2, \quad (1)$$

where E_l and E_s are the incident and scattered photon energies, E_0 is the energy separation between the lowest vibrational levels of the ground and excited electronic states, ω is the resonance Raman shift for LO mode, which is 730 cm^{-1} in our samples, and Γ is homogeneous linewidth. $S = \Delta^2/2$, where Δ is the displacement of ground- and excited-state harmonic surfaces. The index of m shows the vibrational level of ground electronic state takes one and two for fundamental and first overtone phonon correlation.

Values of Γ were estimated from the literature values[31,32] for the homogeneous linewidth at room temperature, while an estimate of E_0 which produced good results in both samples was obtained by averaging the absorption and fluorescence maxima for the ten-dots-in-a-wire sample. Using these values, we find that the above overtone/fundamental ratios can be reproduced with a value of $S = 3.06$ for both samples. Since the Raman intensity ratio is only a weak function of Γ, any resulting error in the inferred value of S is small.[33] Therefore, we can use this value of S for both samples with the same Γ to find their different values of inhomogeneous broadening. For this purpose we use the PL cross section formula[30,34]

$$\sigma_{PL}(E_R) \propto E_R^3 \int_{-\infty}^{+\infty} e^{\frac{1}{\hbar}[i(E_0-E_R)t-\Gamma t-\frac{1}{2\hbar}\Theta^2 t^2]} e^{[-S(1-e^{-i\omega t})]} dt, \quad (2)$$

where E_R is the energy of the emitted photon and Θ is the inhomogeneous linewidth. Values of Θ were obtained as 50 meV and 120 meV for one and ten dot-in-a-wire samples, respectively. With these results, PL spectra were modeled using the same time-dependent theory of Heller *et al.* and using these same calculated parameters obtained from the Raman spectra. The model PL spectra thus obtained showed

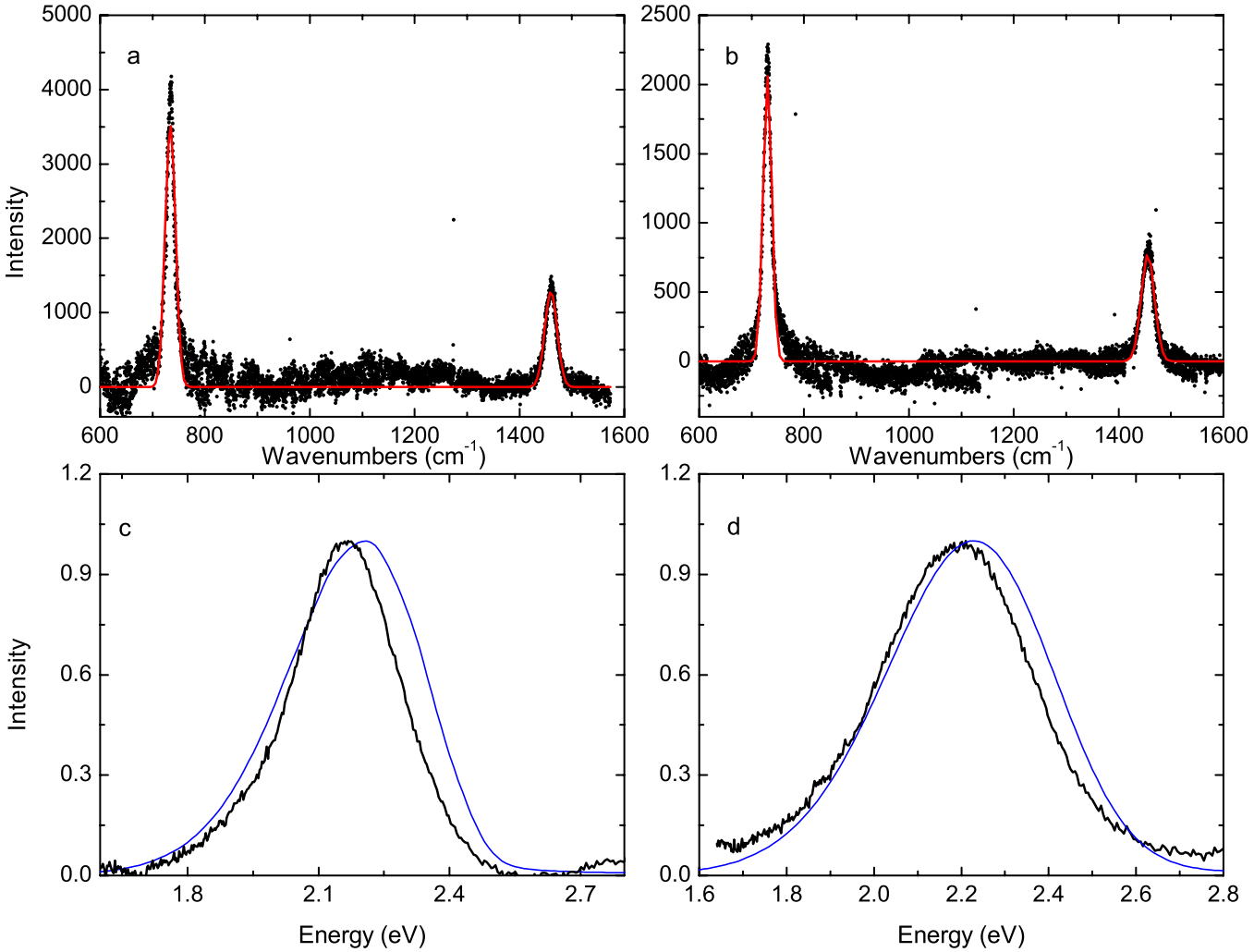

FIG. 4. Raman spectrum fit to a Gaussian is shown in (a) for 1 dot and (b) for 10 dot samples. The PL simulated from the model applied to the Raman data is compared to the PL spectra for 1 and 10 dot samples in (c) and (d). All experimental data are black curves, fits are coloured lines.

good agreement with the experimental results (Figs. 4(c) and 4(d)), providing a consistency check to our work.

We also explored variations of PL properties as a function of excitation position to elucidate the influence of growth conditions on nanowire properties. PL spectra from two different CW excitation sources—xenon lamp and diode laser—with the same excitation wavelength (405 nm) are shown in Fig. 5(a). The PL peak produced by the xenon lamp excitation is broader the one produced by the diode laser, which may be attributable to variations in excitation position and spot size between the two beams.

The samples were fabricated on a circular wafer. The portion analysed was approximately a quarter of the full circle. The variation in PL was systematically investigated by measuring the PL of the ten dots-in-a-wire sample along x, the chord, and y, perpendicular to the chord at 2 mm intervals. As it is shown in Fig. 5(b), there is a decrease of the peak energy of the PL signal from the center to the edge of the wafer. Integrated peak values (not shown) show a similar, decreasing trend; however, FWHM of PL signals show a radial increase from the center to the edge of the sample. These results are consistent with the hypothesis that during synthesis, a radial temperature gradient is present on the substrate surface.[35] This temperature gradient may contribute to the broadening of the overall emission of a single wafer as different regions of the sample way have a higher In content than others. A broad emission bandwidth in the visible spectrum is desirable for white light emission applications.

Figure 6 shows the Commission Internationale de l'Eclairage (CIE) diagrams of the two samples. These spectra give a mathematical description the red-green-blue (RGB) colour spectrum and plot this in the CIE XYZ color space. These plots can be used to determine what perceived color would be emitted from a given PL spectra. The open circles on the respective plots were generated by loading the PL spectra obtained into the CIE algorithm, the resulting circle corresponding to the color of the emission. Both the ten and one dot samples emit in the yellow/green part of the spectrum. This result shows that further control of the temperature gradient can be examined to obtain a dot-in-a-wire LED that is "whiter" according these color specifications.

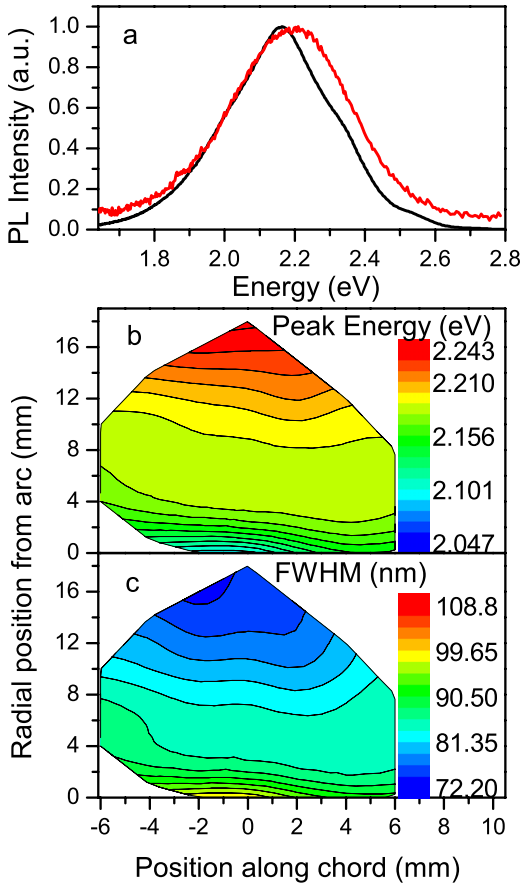

FIG. 5. (a) PL spectra of 10 dot sample with 405 nm diode laser (black dashed line) and 405 nm Xenon lamp (red solid line). (b) Peak PL intensity and (c) FWHM of PL peaks across the sample taken with a 445 nm diode laser.

IV. CONCLUSION

Inhomogeneous broadening caused by incorporating ten InGaN quantum dots in GaN nanowires may be exploited to improve the prospects of nanowire heterostructures as white light sources for LEDs. The integrated peak area and FWHM of the PL signal decreased with temperature. The PL spectra modeled using the parameters calculated from time-dependent theory and Raman intensities showed good agreement with the experimental PL results. A study of the position-dependence of PL shows that the variations in optical properties from center to edge of samples may be attributed to the temperature gradient which occurs in the growth process. To increase PL efficiency, further characterization of the sample will be essential. Time dependent PL spectra, measuring the lifetime of the photoluminescence, will give a better indication of the feasibility of the samples as a white light source. Also, further control over growth conditions will be needed to produces samples with a comparable emission quality to standard warm white color used in conventional lighting.

ACKNOWLEDGMENTS

Financial support from the FQRNT and McGill University is gratefully acknowledged. We thank the McGill University Center for Self-Assembled Chemical Structures for use of their facilities.

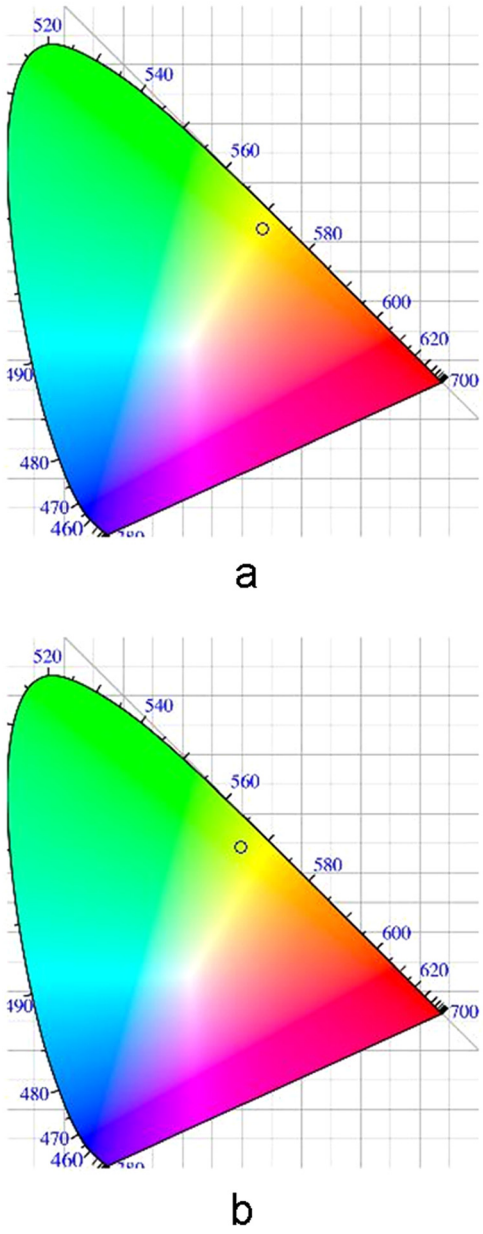

FIG. 6. CIE color spectra of (a) 1 dot and (b) 10 dot samples. Open circle indicated color of emission.

[1]J. Wu, J. Appl. Phys. **106**, 011101 (2009).
[2]R. Yan, D. Gargas, and P. Yang, Nature Photon. **3**, 569 (2009).
[3]M. Yu, Y.-Z. Long, B. Sun, and Z. Fan, Nanoscale **4**, 2783 (2012).
[4]A. I. Hochbaum and P. Yang, Chem. Rev. **110**, 527 (2010).
[5]C. Hahn, Z. Zhang, A. Fu, C. H. Wu, Y. J. Hwang, D. J. Gargas, and P. Yang, ACS Nano **5**, 3970 (2011).
[6]W. Guo, M. Zhang, A. Banerjee, and P. Bhattacharya, Nano Lett. **10**, 3355 (2010).
[7]A. L. Bavencove, G. Tourbot, J. Garcia, Y. Désières, P. Gilet, F. Levy, B. André, B. Gayral, B. Daudin, and D. Le Si, Nanotechnology **22**, 345705 (2011).
[8]F. Qian, Y. Li, S. Gradecak, H.-G. Park, Y. Dong, Y. Ding, Z. L. Wang, and C. M. Lieber, Nature Mater. **7**, 701 (2008).
[9]J. C. Johnson, H.-J. Choi, K. P. Knutsen, R. D. Schaller, P. Yang, and R. J. Saykally, Nature Mater. **1**, 106 (2002).
[10]T. P. Chen, H. Y. Shih, J. T. Lian, J. H. Chen, P. S. Lin, T. Y. Lin, J. R. Gong, and Y. F. Chen, Opt. Express **20**, 17136 (2012).
[11]S. Paul, A. Helwig, G. Müller, F. Furtmayr, J. Teubert, and M. Eickhoff, Sens. Actuators B **173**, 120 (2012).
[12]W. Y. Weng, T. J. Hsueh, S. J. Chang, S. B. Wang, H. T. Hsueh, and G. J. Huang, IEEE J. Sel. Top. Quantum Electron. **17**, 996 (2011).

[13]X. Guo, G. D. Shen, B. L. Guan, X. L. Gu, D. Wu, and Y. B. Li, Appl. Phys. Lett. **92**, 013507 (2008).
[14]V. G. Dubrovskii and N. V. Sibirev, Phys. Rev. B **77**, 035414 (2008).
[15]S. X. Jin, J. Li, J. Z. Li, J. Y. Lin, and H. X. Jiang, Appl. Phys. Lett. **76**, 631 (2000).
[16]A. V. Maslov and C. Z. Ning, Appl. Phys. Lett. **83**, 1237 (2003).
[17]Y. L. Chang, J. L. Wang, F. Li, and Z. Mi, Appl. Phys. Lett. **96**, 013106 (2010).
[18]N. H. P. Trung, C. Kai, Z. Shaofei, F. Saeed, and M. Zetian, Nanotechnology **22**, 445202 (2011).
[19]H. P. T. Nguyen, S. Zhang, K. Cui, X. Han, S. Fathololoumi, M. Couillard, G. A. Botton, and Z. Mi, Nano Lett. **11**, 1919 (2011).
[20]S. Perkowitz, *Optical Characterization of Semiconductors: Infrared, Raman, and Photoluminescence Spectroscopy* (Academic Press, US, 1993).
[21]N. H. P. Trung, D. Mehrdad, C. Kai, and M. Zetian, Nanotechnology **23**, 194012 (2012).
[22]D. Valerini, A. Creti, M. Lomascolo, L. Manna, R. Cingolani, and M. Anni, Phys. Rev. B **71**, 235409 (2005).
[23]S. A. Lourenço, I. F. L. Dias, J. L. Duarte, E. Laureto, V. M. Aquino, and J. C. Harmand, Braz. J. Phys. **37**, 1212 (2007).
[24]D. I. Lubyshev, P. P. Gonzalez-Borrero, J. E. Marega, E. Petitprez, J. N. La Scala, and P. Basmaji, Appl. Phys. Lett. **68**, 205 (1996).
[25]Z. Y. Xu, Z. D. Lu, Z. L. Yuan, X. P. Yang, B. Z. Zheng, J. Z. Xu, W. K. Ge, Y. Wang, J. Wang, and L. L. Chang, Superlattices Microstruct. **23**, 381 (1998).
[26]A. Polimeni, A. Patanè, M. Henini, L. Eaves, and P. C. Main, Phys. Rev. B **59**, 5064 (1999).
[27]D. I. Lubyshev, P. P. Gonzalez-Borrero, E. Marega, E. Petitprez, N. La Scala, and P. Basmaji, Appl. Phys. Lett. **68**, 205 (1996).
[28]F. Limbach, T. Gotschke, T. Stoica, R. Calarco, E. Sutter, J. Ciston, R. Cusco, L. Artus, S. Kremling, S. Hofling, L. Worschech, and D. Grutzmacher, J. Appl. Phys. **109**, 014309 (2011).
[29]S. Hernandez, R. Cusco, D. Pastor, L. Artus, K. P. O'Donnell, R. W. Martin, I. M. Watson, Y. Nanishi, and E. Calleja, J. Appl. Phys. **98**, 013511 (2005).
[30]A. B. Myers, R. A. Mathies, D. J. Tannor, and E. J. Heller, J. Chem. Phys. **77**, 3857 (1982).
[31]G. Christmann, R. Butté, E. Feltin, J. F. Carlin, and N. Grandjean, Phys. Rev. B **73**, 153305 (2006).
[32]T. Tawara, H. Gotoh, T. Akasaka, N. Kobayashi, and T. Saitoh, Phys. Rev. Lett. **92**, 256402 (2004).
[33]T. D. Krauss and F. W. Wise, Phys. Rev. B **55**, 9860 (1997).
[34]T. Petrenko, O. Krylova, F. Neese, and M. Sokolowski, New J. Phys. **11**, 015001 (2009).
[35]J. C. A. Sher, *Physics and Properties of Narrow Gap Semiconductors* (Springer, New York, 2008).